Vertical Structure and Interannual Variability of Tropical Zonal Winds

DAVID S. GUTZLER

Atmospheric and Environmental Research, Inc., Cambridge, Massachusetts

(Manuscript received 25 September 1989, in final form 9 January 1990)

ABSTRACT

Geographical and seasonal variations of the variance and vertical structure of interannual anomalies of seasonally averaged zonal winds are calculated from rawinsonde records at tropical stations between 80°E and 140°W, the longitudes spanned by the "Walker Circulation." Wind anomalies are negatively correlated in the upper and lower troposphere only in a latitude band within about 10° of the equator, defining the latitudinal extent of the Walker Circulation; about 70% of the interannual variance of tropospheric zonal winds is accounted for by a single vertical mode within this band. The band shifts seasonally north and south slightly, in conjunction with seasonal shifts in large-scale convection. The level of zonal overturning occurs between 300 and 500 mb, and is highest near the seasonal convective maximum. Other vertical structures, suggestive of interannual variability not associated with thermally forced circulations, are also found near the equator at some longitudes in the boreal winter season.

1. Introduction

The general tendency for zonal winds in the tropics to have opposite signs in the upper and lower troposphere is well known. In the equatorial zonal plane across the Pacific, the out-of-phase vertical structure of the tropospheric zonal wind field was denoted the "Walker circulation" by Bjerknes (1969), who interpreted it as a direct thermal response to the zonal gradient of sea surface temperature (SST) along the equator in the Pacific. Bjerknes noted that during El Niño warmings in the eastern Pacific both the zonal SST gradient and the Walker circulation are greatly weakened in association with a large scale atmospheric surface pressure fluctuation, the Southern Oscillation (hereafter denoted "SO"; Walker 1924). Subsequent observational studies have verified that zonal wind anomalies associated with extremes of the SO over the tropical Pacific in the upper and lower troposphere tend to have opposite signs (Krueger and Gray 1969; Krueger and Winston 1974; Hastenrath and Wu 1982; Gutzler and Harrison 1987). Bjerknes' concepts have been the foundation for much of the recent research on the causes of El Niño and the SO.

The two-layer structure of the wind field has motivated simplified models of the tropical circulation driven by latent heating. An efficient method of describing the thermally driven flow is to decompose the wind field into vertical normal modes (Matsuno 1966). Gill (1980) used this technique to develop a linear model of the thermally driven flow that includes only the first baroclinic mode of the shallow water equations, with an equal and opposite response in the upper and lower halves of the troposphere. An enhancement of this model has been incorporated into a coupled ocean–atmosphere model used for El Niño forecasts (Cane et al. 1986). Normal mode calculations based on more complete equations have confirmed that much of the variance in the tropics projects onto an internal baroclinic vertical structure (Silva Dias and Bonatti 1985; Nogués-Paegle et al. 1989).

The common use of simple models that simulate only the thermally driven circulation motivates this study of the observed vertical structure of near-equatorial zonal wind anomalies. The first question to be considered is what fraction of the total interannual zonal wind variance is accounted for by out-of-phase fluctuations in the zonal phase. Bjerknes (1969) understood that the Walker circulation is but one part of the total zonal circulation along the equator. In his words, "the zonal wind components in the equatorial vertical profile will be the vectorial sum of the thermally driven circulation . . . plus a field of easterly wind components whose strength depends on the intensity of the divergence of the meridional and vertical fluxes of absolute angular momentum" (Bjerknes 1969). Indeed, Newell et al. (1972) showed that the climatological zonal winds are easterly through the depth of the troposphere across the equatorial western Pacific during northern winter.

In addition to a quantitative verification of the out-of-phase vertical structure of zonal wind anomalies, the results are pertinent to other outstanding issues concerning large-scale, quasi-stationary atmospheric

Corresponding author address: Dr. David S. Gutzler, Atmospheric and Environmental Research, Inc., 840 Memorial Drive, Cambridge, MA 02139.

circulation anomalies in the tropics. These include the seasonality and vertical structure of latent heating, and their effects on convectively forced circulations.

If the out-of-phase structure of interannual wind anomalies is due to the forcing of large-scale equatorial waves by convection, then one might expect the magnitude and structure of the wind anomalies to be modulated by the seasonal cycle of near-equatorial convection. Meehl (1987) showed that SO-associated rainfall anomalies at western Pacific stations are closely coupled to the seasonal cycle of rainfall. Gutzler and Harrison (1987) found that zonal wind anomalies over the far western Pacific associated with SO warm events are weakest in the boreal winter, and pointed out that this might be due to their use of stations north of the equator, which would be only weakly forced by heating centered south of the equator during that season. The vertical structure of the wind field thus provides an index of the seasonality of the Walker circulation.

Details of the vertical structure of the wind field have been related to the vertical structure of latent heating, which is difficult to measure directly. The appropriate choice of vertical structure to use in models where it is prescribed is difficult to determine because the vertical structure of the forcing is not known definitively. In the Gill (1980) model, the forcing is due to the vertical transport of mass associated with large-scale convection, and the vertical velocity is assumed to have a deep vertical distribution peaking in midtroposphere. Some justification for this simple vertical structure was provided by Yanai et al. (1973), who derived a latent heating profile with a broad maximum near 400 mb based on synoptic data from the western Pacific. Houze (1982) used eastern Atlantic data to derive an elevated heating profile with a sharper maximum near 300 mb and no net heating below 500 mb. Hartmann et al. (1984) showed that the Houze (1982) and Yanai et al. (1973) heating profiles produced significantly different zonal wind responses in a linear model, with the elevated heating profile forcing a higher center of overturning.

Previous observational studies of vertical structure have been undertaken with regard to subseasonal variability. Adams (1971) performed an eigenvector decomposition of daily fluctuations of zonal (u) and meridional (v) wind components at several tropical Pacific islands. He found that the dominant eigenvector of Northern Hemisphere summertime v anomalies has a "baroclinic" (out-of-phase) structure. In the Northern winter season, the gravest eigenvector has an "equivalent barotropic" structure, with anomalies of like sign throughout the troposphere.

Concurrent with Adams's study, Madden and Julian (1971) found a broad peak in the variance spectrum of zonal wind fluctuations at stations near the equator around a period of 40–50 days with an out-of-phase vertical structure. Madden (1986), however, subsequently documented seasonal variations in the vertical coherence of 40–50 day bandpass-filtered u fluctuations that are similar to the seasonal differences found by Adams (1971): at western Pacific stations, minimum coherence between 150 mb and 850 mb u anomalies occurs in Northern winter, and maximum (out-of-phase) coherence occurs in Northern summer. Gutzler and Madden (1989) described pronounced geographical and seasonal variations in 40–50 day zonal wind variance, and discussed the possibility of coherent sources of tropical intraseasonal wind variability other than convection.

This paper documents the vertical structure of interannual zonal wind variance across the tropical Indian and western Pacific oceans. Geographical and seasonal differences in the variance and vertical structure of seasonally averaged anomalies are examined and interpreted in terms of numerical studies, and compared with statistics of higher frequency variability.

2. Data and analysis procedures

This study is based on a subset of the rawinsonde dataset used by Gutzler (1987) to describe the annual and semiannual cycles of tropical winds. Monthly averaged rawinsonde observations were obtained from *Monthly Climatic Data for the World,* archived by the Data Support Section at the National Center for Atmospheric Research. This study uses time series from 18 stations (see Fig. 1) between 25°S and 25°N latitude and ranging in longitude from about 80°E eastward to about 140°W, the region spanned by the Walker Circulation (Bjerknes 1969; Newell et al. 1972, 1974). Data at six levels (850, 700, 500, 300, 200, and 150 mb) are considered. The data record extends through the end of 1980; more than 15 years of data are present in the record for most stations and seasons. Gutzler (1987) describes the quality-checking procedures applied to the monthly mean data.

Extension and verification of the results presented here can eventually be made using analysis products, which potentially afford much better horizontal resolution than the rawinsonde network allows. Except at

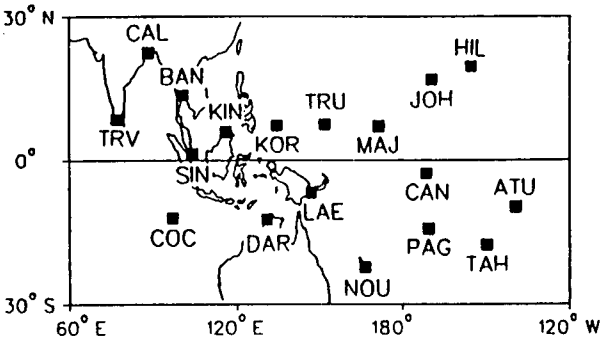

FIG. 1. Map of station locations. Unabbreviated station names are given in Table 1 of Gutzler (1987).

a few data-rich levels, however, an analysis may be severely constrained by the particular interpolation and assimilation procedures used, and changes in analysis procedures may contaminate temporal variations in the observations. Direct use of time-averaged rawinsonde data was judged preferable for studying the vertical structure of the tropospheric circulation.

To minimize spurious interannual variability due to aliasing of variance associated with the 40–50 day oscillation in the time-averaged winds, the monthly mean data have been averaged into seasonal means (Gray and Madden 1986). Months were grouped into seasons in standard fashion: December–January–February (DJF), March–April–May (MAM), June–July–August (JJA), and September–October–November (SON). If one month is missing from a season, the seasonal mean refers to an average over the two available monthly means with climatology (i.e., zero anomaly) assumed for the missing month. No seasonal mean is calculated if two or three months are missing. Climatological means are calculated for each station, pressure level, and season, and are then subtracted from each seasonal average to produce time series of seasonal anomalies.

The vertical structure of interannual zonal wind fluctuations is examined first by correlating seasonal anomalies at different pressure levels at each station. Correlations exceeding |0.6| are emphasized. These satisfy a 5% significance threshold, using a two-tailed t-test conservatively assuming ten degrees of freedom (the number of degrees of freedom varies from station to station, and the test is applied here nonrigorously on an a posteriori basis).

The vertical structure is then described in more detail using eigenvector analysis (also called empirical orthogonal function or EOF analysis). The EOFs in this paper are the eigenvectors of the mass-weighted covariance matrix of wind fluctuations at the six levels, as described by Gutzler and Harrison (1987), calculated separately for each station and season. These calculations are analogous to those performed by Adams (1971) on daily meridional wind anomalies in the tropics. The statistical significance of the eigenvectors is assessed by applying a rule-of-thumb for nondegeneracy (North et al. 1982) to the first and second eigenvalues. The first eigenvalue satisfies this test for all but one of the eigenvectors shown. The single exception occurs at the station with the shortest period of record, and although the significance tests take into account the length of each time series, the limited period of record remains a general limitation of this study.

It is expected that the Southern Oscillation will be highly correlated with the wind fluctuations under study. Such correlations are well established (e.g., Kidson 1975; Arkin 1982; Horel 1982; Selkirk 1984), so statistics derived directly on the basis of a Southern Oscillation Index are not emphasized in this study, although some of the results are interpreted in terms of the evolution of SO phenomena documented previously.

3. Interannual variability

In this section the geographical and seasonal variations of zonal wind variance and its vertical structure are compared. Emphasis is placed on a comparison of results for SON and DJF, which exemplify the results for other seasons.

Figure 2 contains plots of the interannual standard deviation [denoted $\sigma(u_l)$, where l is the pressure level] of SON seasonal zonal wind anomalies at 850 mb and 200 mb. At 850 mb, maximum interannual standard deviations of about 2 m s^{-1} are found across the near-equatorial western Pacific from Singapore eastward to Canton, the region studied in detail by Gutzler and Harrison (1987). To the north and south of this line of stations $\sigma(u_{850})$ drops to less than 1 m s^{-1}. The magnitude and geographical distribution of $\sigma(u_{200})$ are quite different. Maximum standard deviations are found over the south central Pacific where $\sigma(u_{200})$ ex-

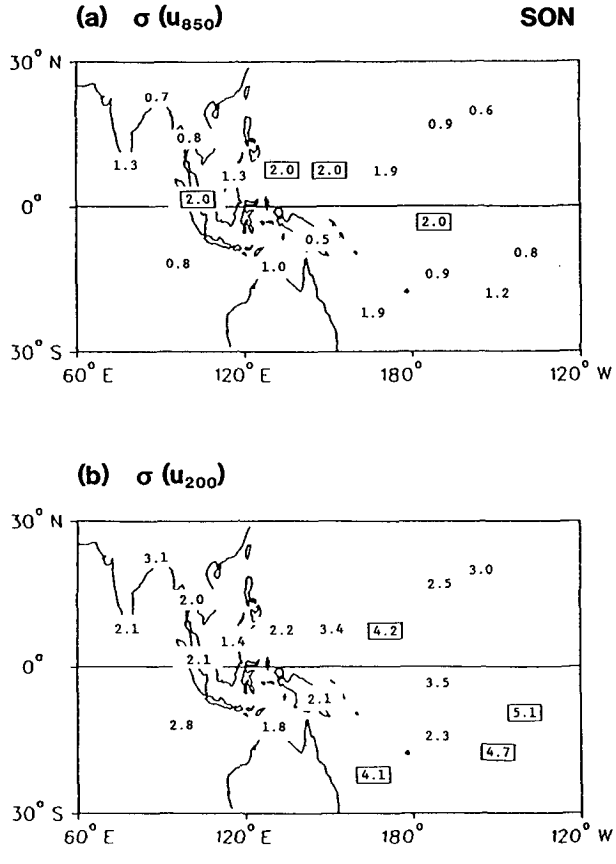

FIG. 2. Standard deviation (units m s^{-1}) of seasonally averaged anomalies of the zonal wind at each station for SON. (a) 850 mb: a solid box is drawn around values greater than or equal to 2.0 m s^{-1}. (b) 200 mb: a solid box is drawn around values greater than or equal to 4.0 m s^{-1}.

ceeds 4 m s^{-1}. At stations poleward of 10° in both hemispheres, standard deviations are several times larger at 200 mb relative to 850 mb. At near-equatorial stations west of 150°E, however, $\sigma(u_{200}) \approx \sigma(u_{850}) \approx 2$ m s^{-1}.

The complete set of vertical correlations $r(u_l, u_m)$ is summarized in Fig. 3 by showing just two plots: $r(u_{200}, u_{500})$, representative of upper tropospheric coupling, and $r(u_{200}, u_{850})$, representative of coupling through nearly the entire depth of the troposphere. Significant positive values of $r(u_{200}, u_{500})$ are observed at stations poleward of 10° in both hemispheres. Large negative values of $r(u_{200}, u_{850})$ are found at near-equatorial Indian and western Pacific stations, including most of the stations where $\sigma(u_{850})$ is large. Correlations $r(u_{200}, u_{850})$ exceeding |0.6| are almost all negative, whereas values of $r(u_{200}, u_{500})$ exceeding that threshold are all positive. Furthermore, with very few exceptions $r(u_{200}, u_{850})$ is small at stations where $r(u_{200}, u_{500})$ is large, and $r(u_{200}, u_{850})$ is large at stations where $r(u_{200}, u_{500})$ is small. The correlations at Canton and Atuona, east of the date line, are exceptional in that both $r(u_{200}, u_{500})$ and $r(u_{200}, u_{850})$ are significantly different from zero with opposite signs.

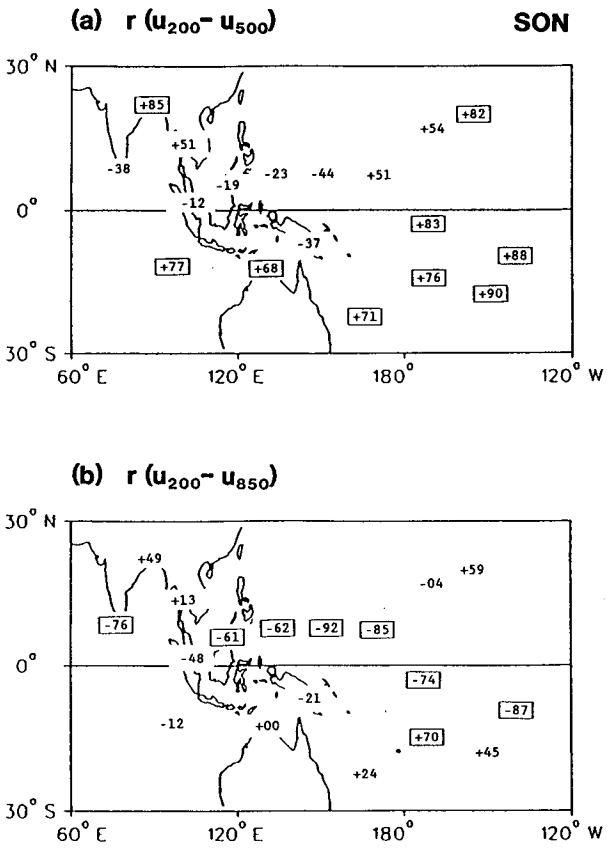

FIG. 3. (a) Correlation between SON seasonal anomalies of the zonal wind at 500 mb and 200 mb at each station. A solid box is drawn around correlation coefficients exceeding 0.6 in magnitude. (b) As in panel (a) but for the correlation between SON seasonal anomalies of the zonal wind at 850 mb and 200 mb at each station.

Large negative values of $r(u_{200}, u_{850})$ are representative of a deep, out-of-phase vertical structure of interannual zonal wind anomalies. From Fig. 3b it can be seen that such a structure is characteristic of zonal anomalies only within about 10° of the equator. This latitude marks the approximate poleward limit of the dominance of out-of-phase zonal circulations. Several stations in the far western near-equatorial Pacific have nearly equal standard deviations in upper and lower tropospheric zonal winds, which together with the observed out-of-phase vertical structure suggests that 2 m s^{-1} is an appropriate amplitude for the purely convectively forced component of interannual zonal wind variability.

Large positive values of $r(u_{200}, u_{500})$ are suggestive of equivalent barotropic fluctuations and are often interpreted as such, but external modes would exhibit large positive values of $r(u_{200}, u_{850})$ as well (found only at Pago Pago in the southwest Pacific). Most of the $r(u_{200}, u_{850})$ values in Fig. 3b are small, suggesting that the wind fluctuations away from the near-equatorial center of convective variability are really vertically decoupled (Charney 1963), or that the correlations reflect a combination of out-of-phase and in-phase fluctuations whose sum is vertically incoherent.

Figure 4 presents a more detailed picture of vertical coherence derived from eigenvector analyses carried out at each station based on the covariances among SON u anomalies at all six pressure levels in the dataset. The figure thus depicts geographical variations of the dominant vertical structure of u anomalies at each station and the relative amplitudes of u anomalies described by the dominant vertical structure. The fraction of variance accounted for by the first eigenvector seems to be positively correlated with the interannual variance of u_{200}, i.e., tropospheric u fluctuations at stations where $\sigma(u_{200})$ is large can be efficiently described in terms of a single vertical profile. This may simply be the result of larger upper tropospheric wind anomalies dominating the eigenvectors of the u covariance matrix, although the mass-weighting should counteract this tendency. It is also possible that upper tropospheric anomalies are generally more representative of deep structure (either in-phase or out-of-phase) than are lower tropospheric anomalies.

Each of the eigenvectors can be characterized as having either an in-phase or an out-of-phase structure. The geographical distribution of these structures in Fig. 4 is broadly consistent with the inferences made from the correlation plots in Fig. 3. In addition, the "node level" of the out-of-phase eigenvectors (the level at which the eigenvector changes sign) may provide some suggestion as to the vertical structure of the heating. For interannual u anomalies during SON, the node

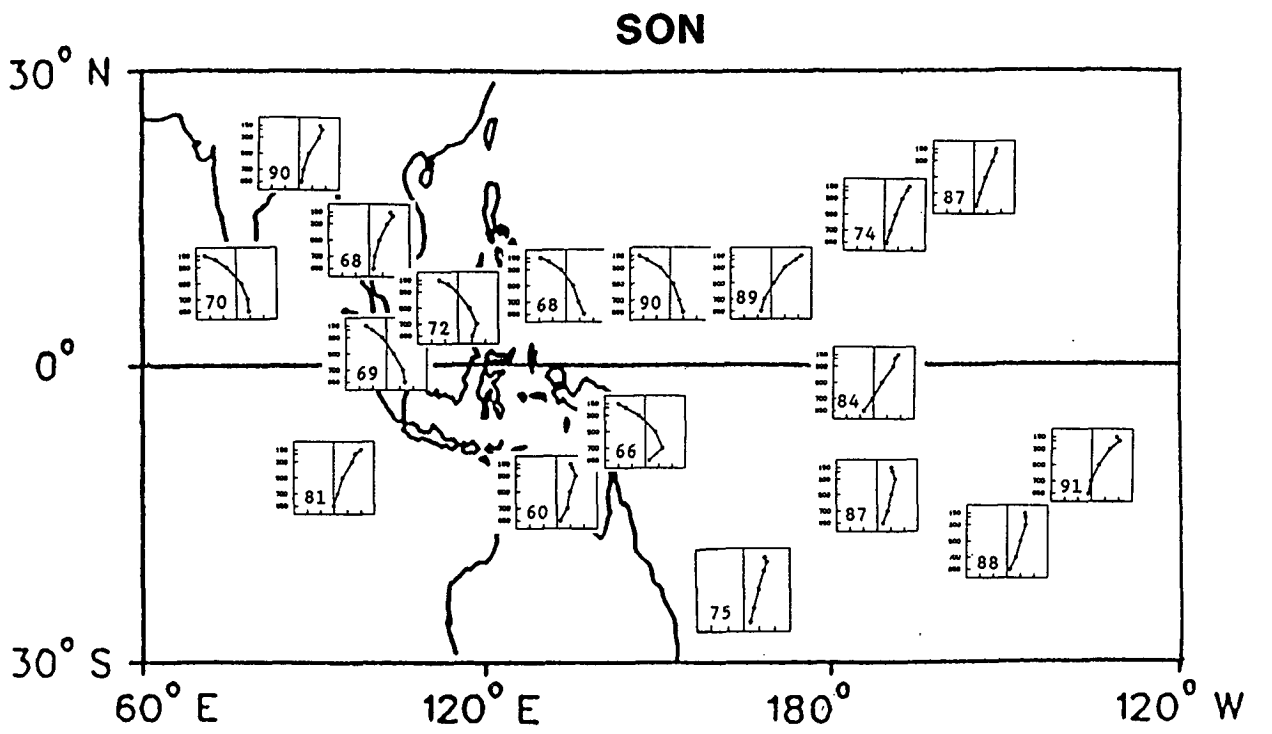

FIG. 4. Gravest eigenvector of the vertical profile of SON seasonal zonal wind anomalies at each station. Each eigenvector is normalized; the scale and the sign of each eigenvector are arbitrary. The number in the lower left corner of each eigenvector is the percentage of total mass-weighted variance accounted for by the eigenvector. Each eigenvector is nondegenerate based on the rule of thumb of North et al. (1982).

level is highest (close to 300 mb) at stations across the far western near-equatorial Pacific (Singapore, Kota Kinabalu, and Koror). Moving westward from Singapore or eastward from Koror, the node level is closer to 500 mb. East of Truk the node level drops to between 500 mb and 700 mb. Thus $r(u_{200}, u_{500})$ is typically small where an out-of-phase structure predominates because 500 mb is just below the midtropospheric node, except at the stations farthest to the east (Canton and Atuona) where 500 mb is above the node level.

Figure 5 contains plots of the interannual standard deviation of zonal wind anomalies at 850 mb and 200 mb for DJF, analogous to the plots in Fig. 2 for SON. The standard deviations at stations west of the date line in the Pacific are greatly reduced relative to SON in both the upper and lower troposphere. At stations north of the equator between Singapore and the date line, where Gutzler and Harrison (1987) found only weak tropospheric zonal wind anomalies associated with SO warm events during DJF, $\sigma(u_{850})$ is only about half of its SON value. At Southern Hemisphere stations, however, $\sigma(u_{850})$ is larger in DJF compared with SON. Interannual variability in the upper troposphere is much larger in DJF than in SON at stations poleward of 10° in both hemispheres. Values of $\sigma(u_{200})$ increase rapidly poleward, in contrast to the small latitudinal gradients of $\sigma(u_{850})$. Thus the lower tropospheric variance is consistent with the seasonal shift of convective forcing into the Southern Hemisphere between SON and DJF, but upper tropospheric variances off the equator are greater in DJF in both hemispheres.

Vertical correlations among u_{850}, u_{500}, and u_{200} for DJF are shown in Fig. 6. Most of the $r(u_{200}, u_{850})$ values across the western near-equatorial Pacific are considerably lower than the SON values, but correlations at South Pacific stations are significantly negative. At the two Indian stations both $r(u_{200}, u_{500})$ and $r(u_{200}, u_{850})$ are significantly positive, indicating that wintertime interannual wind variability is strongly equivalent barotropic. Upper tropospheric vertical coupling in DJF is stronger in the Northern Hemisphere and weaker in the near-equatorial Southern Hemisphere relative to SON. Values of $r(u_{200}, u_{850})$ at stations in the South Pacific poleward of 15°S are significantly positive in both seasons. In general the in-phase signature is stronger and the out-of-phase signature is weaker in DJF than in SON.

Vertical eigenvectors for the DJF season are shown in Fig. 7. The node level of out-of-phase eigenvectors reaches its maximum (slightly above the 300 mb level) at Darwin, Lae, and Koror, and drops to the east and west of those stations, similar to the SON results. In each of these seasons, the region of highest node level is located near the seasonal convective maximum

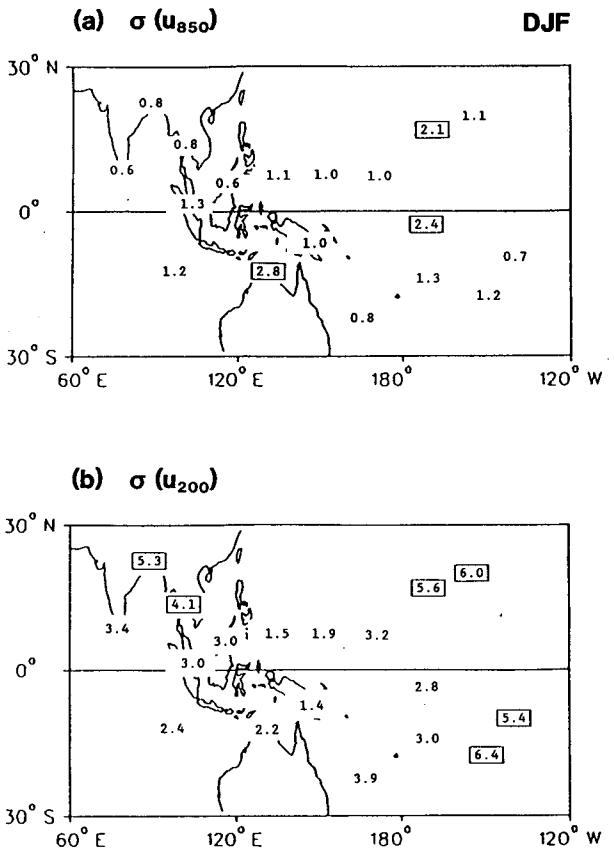

FIG. 5. As in Fig. 2 but for DJF.

(Meehl 1987). The node level is therefore highest near the center of convective forcing and drops to the east and west of the forcing.

At Truk and Majuro (at 7°N just west of the date line), the eigenvectors have an in-phase structure instead of the out-of-phase structure typical of other stations equatorward of 10°. At these stations $\sigma(u_{200})$ is considerably larger than $\sigma(u_{850})$ (Fig. 5) and u anomalies are positively correlated throughout the troposphere (Fig. 6). Taken together these results suggest that considerable interannual variance over the near-equatorial western Pacific in DJF is associated with barotropic processes rather than equatorial convective forcing.

One possible source of such variability is equatorward-propagating Rossby waves. To compare the coherence of interannual zonal wind variability at Majuro with extratropical and equatorial fluctuations, seasonal averages of the 200 mb zonal wind at Kagoshima, Japan (31.6°N, 130.6°E) are used as an index of interannual fluctuations of the subtropical jet in boreal winter. Correlations among this index, the Tahiti–Darwin Southern Oscillation Index (SOI), and the zonal wind at Majuro were calculated. Interannual fluctuations of u_{200} at Majuro are comparably correlated with the speed of the jet (−0.48) and with the SOI (+0.42), whereas the correlation between the jet speed and the SOI is nearly zero (+0.16). Thus the interannual variability of the 200 mb zonal wind at Majuro is independently correlated with the SOI and with the speed of the subtropical jet, providing some evidence of tropical–extratropical interaction that may not be directly related to SO fluctuations.

The geographical distributions of $\sigma(u_{850})$ and $\sigma(u_{200})$ for MAM are shown in Fig. 8. Across most of the western near-equatorial Pacific, both $\sigma(u_{850})$ and $\sigma(u_{200})$ are less than 2 m s^{-1}. Largest values of $\sigma(u_{200})$, between 4 and 5 m s^{-1}, are found at Pacific subtropical stations in both hemispheres. The pattern of standard deviations at both levels is nearly symmetric about the equator. Thus at near-equatorial stations the interannual variance of zonal winds is less in MAM than in SON, the other equinoctial season, whereas poleward of 10° the interannual variance is about the same for the two seasons.

Interannual variability during JJA (Fig. 9) is also small. At 850 mb, $\sigma(u)$ exceeds 1.5 m s^{-1} only at Koror, Truk, and Noumea. At 200 mb, $\sigma(u)$ exceeds 3 m s^{-1} only at Hilo and Atuona. The principal difference between the JJA and MAM results is the smaller JJA variances at central Pacific stations. Small variance in JJA relative to other seasons is also characteristic of

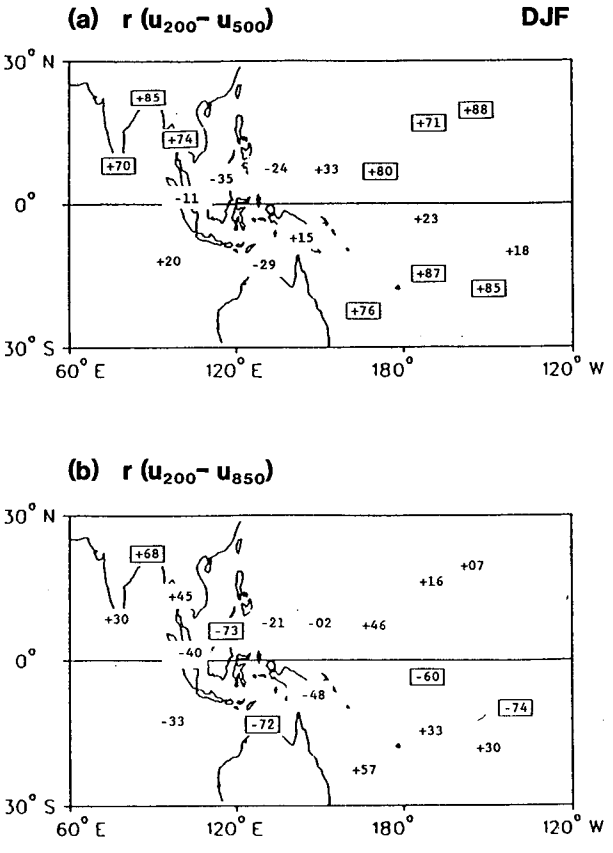

FIG. 6. As in Fig. 3 but for DJF.

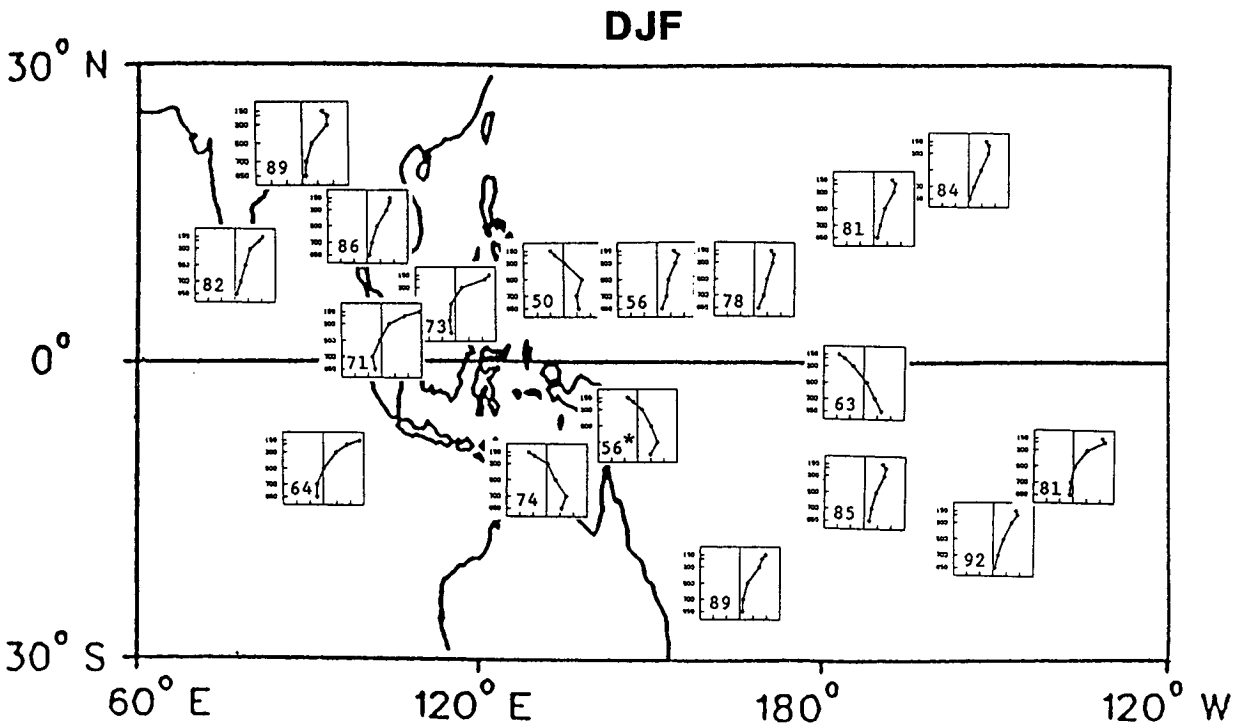

FIG. 7. As in Fig. 4 but for DJF. The eigenvector at Lae (whose fractional variance is denoted by an asterisk) does not satisfy the North et al. (1982) test for nondegeneracy, which is satisfied by the eigenvector at all other stations.

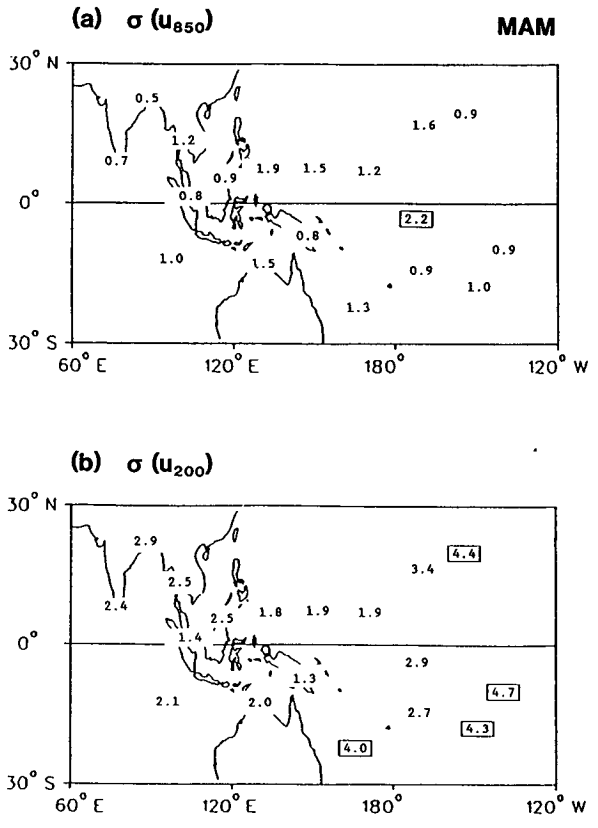

FIG. 8. As in Fig. 2 but for MAM.

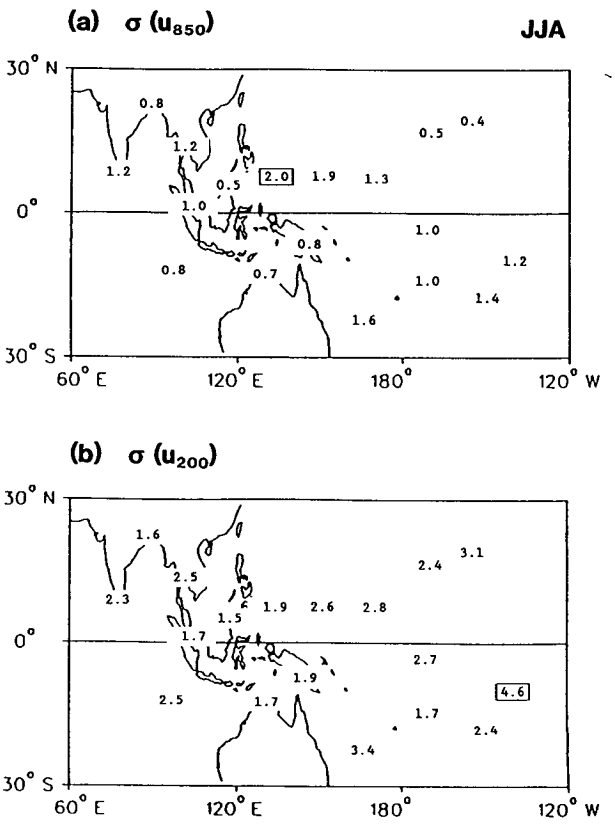

FIG. 9. As in Fig. 2 but for JJA.

TABLE 1. Summary of u_{850} and u_{200} interannual variability. The 18 stations have been grouped into two groups of 9 stations each: "near-equatorial" stations, located within 10° of the equator, and "off-equatorial" stations, located poleward of 10° in either hemisphere. The entries in the table are the root-mean-square averages (m s^{-1}) of the interannual standard deviations of zonal wind anomalies among stations in the group.

		SON	DJF	MAM	JJA
Near-equatorial	$\sigma(u_{850})$	1.6	1.2	1.3	1.3
	$\sigma(u_{200})$	3.1	3.0	2.5	2.6
Off-equatorial	$\sigma(u_{850})$	1.0	1.5	1.1	1.0
	$\sigma(u_{200})$	3.0	4.6	3.3	2.4

intraseasonal zonal wind fluctuations (Madden 1986). Vertical correlations and eigenvectors for MAM and JJA (not shown) corroborate the change from in-phase to out-of-phase vertical structure at about 10° latitude.

Seasonal variations of interannual u variance across the tropical western Pacific and eastern Indian oceans are summarized in Table 1. Based on the maps shown in Figs. 2, 5, 8, and 9, the 18 stations were divided into two 9-station groups: a near-equatorial group including all stations within 10° of the equator, and an off-equatorial group which includes all stations poleward of 10° in both hemispheres. The table presents the interannual u variance at 850 mb and 200 mb averaged over these groups for each season. The near-equatorial group is characterized by maximum variance in SON and minimum variance in MAM and JJA, with the SON maximum most pronounced at 850 mb. The off-equatorial group shows different and stronger seasonal contrasts, including a distinct DJF maximum at both levels and minimum variance in JJA. The DJF maximum is found at stations in both hemispheres (Fig. 5b), not just the winter (Northern) hemisphere. The geographical and seasonal variations of $\sigma(u_{850})$ and $\sigma(u_{200})$ are very similar to those described by Madden (1986) and Gutzler and Madden (1989) for 40–50 day filtered zonal winds.

4. Discussion

The Walker circulation as conceived by Bjerknes (1969), featuring a large-scale zonal overturning in the equatorial plane over the western Pacific, is consistent with the observed structure of interannual zonal wind variance within about 10° of the equator. An out-of-phase vertical structure accounts for about 70% of the variability of zonal winds over the western near-equatorial Pacific. Even within this region, however, the node level of zonal overturning varies so a fixed vertical structure can only approximate the observations.

The vertical structure of interannual zonal wind fluctuations changes at about 10° latitude to an in-phase vertical structure in both hemispheres. The latitudinal distribution of out-of-phase vertical profile predominance can be interpreted in terms of equatorially trapped stationary circulations forced by seasonal anomalies of latent heating. Gill (1980) showed that the appropriate latitudinal length scale for stationary solutions on the equatorial β-plane is a Rossby radius y_E, defined as

$$y_E = \left(\frac{c}{2\beta}\right)^{1/2} = \frac{(gh)^{1/4}}{(2\beta)^{1/2}}$$

where h is the shallow water equivalent depth, β is the meridional gradient of the Coriolis parameter df/dy, g is gravitational acceleration, and c is the shallow water wave speed $\sqrt{gh}$. For an equivalent depth of 350 m, appropriate for a response extending through the depth of the troposphere, Gill found $y_E \approx 10°$ latitude, in close agreement with the latitudinal extent of out-of-phase vertical profile predominance found in this study. Note that this result is not very sensitive to the choice of equivalent depth because y_E is proportional to the fourth root of h.

The latitudinal band of strongest out-of-phase vertical coupling shifts north and south with season, following the zone of most intense convection and convection anomalies. The vertical structure changes altogether with season at several near-equatorial stations west of the date line in the Northern Hemisphere, where an out-of-phase structure accounts for most of the variance in the SON season but an in-phase structure dominates in DJF.

To a large degree these seasonal variations can be interpreted in terms of the seasonal phase-locking characteristic of the evolution of Southern Oscillation phenomena. The SOI typically reaches its most extreme values during the SON season (Rasmusson and Carpenter 1982). The large variance and strong out-of-phase vertical coupling evident in SON at stations across the near-equatorial western Pacific is consistent with other studies that show strong SO signals during that season. Correlations between u_{200} over the western Pacific and the SOI are higher in SON than in other seasons (Selkirk 1984). Gutzler and Harrison (1987) showed that zonal wind anomalies over the far western Pacific Ocean display a characteristic pattern in the SON season preceding the onset of El Niño, with anomalies nearly as large (and opposite in sign) as the anomalies that occur one year later during the mature phase of a warm event.

In contrast, the relatively low interannual variance in MAM is consistent with the observation that only one MAM season falls within the canonical 18-month lifecycle of an SO warm event (Rasmusson and Carpenter 1982). The phase-locked nature of these events thus results in a significant asymmetry of interannual variance near the equator during the two equinoctial seasons. Poleward of 10°, however, the interannual variance is about the same in these two seasons.

The node level of out-of-phase eigenvectors generally

occurs between 300 mb and 500 mb, with the highest node levels (near 300 mb) found at stations in the far western Pacific where the first eigenvector accounts for the highest percentage of variance, i.e., wind fluctuations there are almost entirely out-of-phase in character. Modeling studies indicate that the node level might provide a sensitive indication of the vertical structure of latent heating. As discussed in the Introduction, various simple models using several different heating profiles yield widely varying node levels. The eigenvector results and the vertical correlations in the wind field shown here indicate that the level of sign reversal in seasonal zonal wind anomalies is between 500 and 300 mb, more closely resembling the response calculated by Hartmann et al. (1984) to an elevated heating profile (Houze 1982) than the response to a broader heating profile (Yanai et al. 1973).

A plausible interpretation of the variation with longitude of the node level is inferred from studies of Simmons (1982) and Held (1983). In their models, forcing applied in the tropics generates a set of modes with different vertical wavelengths. Shallow modes propagate vertically more rapidly than deep modes, so the deepest modes predominate at distances far from the forcing region. Convection over the tropical Pacific in the SON season is greatest near Borneo (Janowiak et al. 1985; Meehl 1987). This convective maximum tends to be enhanced during the SON season prior to El Niño and depressed during SON of an El Niño year. If we regard Borneo to be the center of the forcing region for SON interannual variability, then the vertical structure at stations nearest Borneo (Kota Kinabalu and Singapore) can be interpreted as representing the response to latent heating within the forcing region. These stations exhibit the highest node level. The node level drops at stations to the east and west of the forcing region; east of the date line and poleward of 10° the vertical structure starts to resemble an external mode.

Interannual zonal wind variance near the equator with an in-phase vertical structure is most evident over the western Pacific north of the equator in the DJF season, the same location and season for which Adams (1971) and Madden (1986) found evidence for equivalent barotropic structures in intraseasonal fluctuations. Rossby waves propagating equatorward from the extratropics have similar vertical structures, and the observed correlation between seasonal anomalies of the subtropical jet speed and u_{200} at Majuro is consistent with this concept. The climatological zonal wind field, however, is easterly at all levels over the near-equatorial western Pacific in DJF, which should inhibit such propagation (Webster and Holton 1982; Held 1983). Furthermore, the upper tropospheric meridional winds over this region are southerly, which should enhance transmission of northward-propagating Rossby waves and inhibit transmission of southward-propagating Rossby waves (Schneider and Watterson 1984), also arguing against a Northern Hemisphere energy source. Alternatively, zonal wind anomalies with an in-phase vertical structure at the equator near the date line could be achieved by shifting the climatological stationary wave pattern east or west.

A general result of this analysis, then, is that the approximation of the tropical zonal wind circulation as an deep zonal overturning forced by convection over the western Pacific (Gill 1980) gets worse the farther one moves away from the region of maximum convection. Because this analysis focuses on the wind field in the vicinity of the western Pacific convective maximum, however, many features of the distant near-equatorial response to interannual fluctuations in convection are not addressed. Other datasets and analysis techniques are better suited to that purpose.

Acknowledgments. The core of this research was carried out at the MIT Center for Meteorology and Physical Oceanography as part of the author's Ph.D. dissertation. Heartfelt thanks are extended to Dr. D. E. Harrison, who supervised the dissertation and provided a patient ear and unflagging encouragement. Prof. J. M. Wallace brought Adams's thesis to my attention. Dr. R. D. Rosen provided a helpful review of the manuscript. This material is based upon work supported by the National Science Foundation under Grants OCE-83-01787 and ATM-86-13060, and by the U.S. TOGA Project Office under NOAA Contract NA88AA-D-AC038.

REFERENCES

Adams, H. A., 1971: The application of empirical orthogonal functions to meteorological fields in the tropical western Pacific. M.S. thesis, University of Washington, 86 pp.

Arkin, P. A., 1982: The relationship between interannual variability in the 200 mb tropical wind field and the Southern Oscillation. *Mon. Wea. Rev.*, **110,** 1393–1404.

Bjerknes, J., 1969: Atmospheric teleconnections from the equatorial Pacific. *Mon. Wea. Rev.*, **97,** 163–172.

Cane, M. A., S. E. Zebiak and S. C. Dolan, 1986: Experimental forecasts of El Niño. *Nature,* **321,** 827–832.

Charney, J. G., 1963: A note on large-scale motions in the tropics. *J. Atmos. Sci.*, **20,** 607–609.

Gill, A. E., 1980: Some simple solutions for heat-induced tropical circulation. *Quart. J. Roy. Meteor. Soc.*, **106,** 447–462.

Gray, B. M., and R. A. Madden, 1986: Aliasing in time-averaged tropical pressure data. *Mon. Wea. Rev.*, **114,** 1618–1622.

Gutzler, D. S., 1987: The annual and semiannual cycles of the tropical wind field. *Mon. Wea. Rev.*, **115,** 2553–2564.

——, and D. E. Harrison, 1987: The structure and evolution of seasonal wind anomalies over the eastern Indian and western Pacific oceans. *Mon. Wea. Rev.*, **115,** 169–192.

——, and R. A. Madden, 1989: Seasonal variations in the spatial structure of intraseasonal tropical wind fluctuations. *J. Atmos. Sci.*, **46,** 641–660.

Hartmann, D. L., H. H. Hendon and R. A. Houze, 1984: Some implications of the mesoscale circulations in tropical cloud clusters for large-scale dynamics and climate. *J. Atmos. Sci.*, **41,** 113–121.

Hastenrath, S., and M. C. Wu, 1982: Oscillations of upper-air circulation and anomalies in the surface climate of the tropics. *Arch. Meteor. Geophys. Bioklim., Ser. B,* **31,** 1–37.

Held, I., 1983: Stationary and quasi-stationary eddies in the extratropical atmosphere: Theory. *Large-Scale Dynamical Processes*

in the Atmosphere, B. J. Hoskins and R. P. Pearce, Eds., Academic Press, 127–168.

Horel, J. D., 1982: On the annual and interannual variations of the tropical Pacific atmosphere and ocean. Ph.D. dissertation, University of Washington, 136 pp.

Houze, R. A., 1982: Cloud clusters and large-scale vertical motions in the tropics. *J. Meteor. Soc. Jpn.,* **60,** 396–410.

Janowiak, J. E., A. F. Krueger, P. A. Arkin and A. Gruber, 1985: Atlas of outgoing longwave radiation derived from NOAA satellite data. *NOAA Atlas No. 6,* U.S. Dept. of Commerce, 44 pp.

Kidson, J. W., 1975: Tropical eigenvector analysis and the Southern Oscillation. *Mon. Wea. Rev.,* **103,** 187–196.

Krueger, A. F., and T. I. Gray, 1969: Long term variations in equatorial circulation and rainfall. *Mon. Wea. Rev.,* **97,** 700–711.

——, and J. S. Winston, 1974: A comparison of the flow over the tropics during two contrasting circulation regimes. *J. Atmos. Sci.,* **31,** 358–370.

Madden, R. A., 1986: Seasonal variations of the 40–50 day oscillation in the tropics. *J. Atmos. Sci.,* **43,** 3138–3158.

——, and P. R. Julian, 1971: Detection of a 40–50 day oscillation in the zonal wind in the tropical Pacific. *J. Atmos. Sci.,* **28,** 702–708.

Matsuno, T., 1966: Quasi-geostrophic motions in the equatorial area. *J. Meteor. Soc. Jpn., Ser. II,* **44,** 25–43.

Meehl, G. A., 1987: The annual cycle and interannual variability in the tropical Pacific and Indian Ocean regions. *Mon. Wea. Rev.,* **115,** 27–50.

Newell, R. E., J. W. Kidson, D. G. Vincent and G. J. Boer, 1972: *The General Circulation of the Tropical Atmosphere and Interactions with Extratropical Latitudes,* Vol. 1, Massachusetts Institute of Technology Press, 258 pp.

——, ——, —— and ——, 1974: *The General Circulation of the Tropical Atmosphere and Interactions with Extratropical Latitudes,* Vol. 2, Massachusetts Institute of Technology Press, 371 pp.

Nogués-Paegle, J., B.-C. Lee and V. E. Kousky, 1989: Observed modal characteristics of the intraseasonal oscillation. *J. Climate,* **2,** 496–507.

North, G. R., T. L. Bell, R. F. Cahalan and F. J. Moeng, 1982: Sampling errors in the estimation of empirical orthogonal functions. *Mon. Wea. Rev.,* **110,** 699–706.

Oort, A. H., 1983: Global atmospheric circulation statistics, 1958–1973. NOAA Prof. Pap. 14, U.S. Dept. of Commerce, 180 pp.

Rasmusson, E. M., and T. H. Carpenter, 1982: Variations in tropical sea surface temperature and surface wind fields associated with the Southern Oscillation/El Niño. *Mon. Wea. Rev.,* **110,** 354–384.

Schneider, E. K., and I. G. Watterson, 1984: Stationary Rossby wave propagation through easterly layers. *J. Atmos. Sci.,* **41,** 2069–2083.

Selkirk, R., 1984: Seasonally stratified correlations of the 200 mb tropical wind field to the Southern Oscillation. *J. Climatol.* **4,** 365–382.

Silva Dias, P., and J. P. Bonatti, 1985: A preliminary study of the observed vertical mode structure of the summer circulation over tropical South America. *Tellus,* **37,** 185–195.

Simmons, A. J., 1982: The forcing of stationary wave motion by tropical diabatic heating. *Quart. J. Roy. Meteor. Soc.,* **108,** 503–534.

Walker, G. W., 1924: Correlation in seasonal variations of weather. IX: A further study of world weather. *Mem. Indian Meteor. Dept.,* **24,** 275–332.

Webster, P. J., and J. R. Holton, 1982: Cross-equatorial response to middle-latitude forcing in a zonally varying basic state. *J. Atmos. Sci.,* **39,** 722–733.

Yanai, M., S. Esbensen and J.-H. Chu, 1973: Determination of bulk properties of tropical cloud clusters from large-scale heat and moisture budgets. *J. Atmos. Sci.,* **30,** 611–627.